HHS Public Access

Author manuscript

Chem Biol Drug Des. Author manuscript; available in PMC 2023 April 25.

Published in final edited form as:

Chem Biol Drug Des. 2022 April ; 99(4): 620–633. doi:10.1111/cbdd.14030.

1,3-Diarylpyrazolones as Potential Anticancer Agents for Non-Small Cell Lung Cancer: Synthesis and Antiproliferative Activity Evaluation

Achyut Dahal[2], **Mary Lo**[1], **Sitanshu Singh**[2], **Huu Vo**[1], **Denzel ElHage**[1], **Seetharama D. Jois**[2], **Siva Murru**[1]

[1]School of Sciences, College of Arts, Education & Sciences, University of Louisiana Monroe, Monroe, LA 71201.

[2]School of Basic Pharmaceutical and Toxicological Sciences, College of Pharmacy, University of Louisiana Monroe, Monroe, LA, 71201.

Abstract

A series of pyrazolone compounds with different substitution patterns have been synthesized using microwave assisted methods and evaluated their in vitro antiproliferative activity against human lung adenocarcinoma cell lines (A549 and NCI-H522). Among the tested compounds, the pyrazolone P7 exhibited high antiproliferative activity against both A549 and NCIH522 cancer cell lines while being 10 times less cytotoxic to non-cancerous cells. Moreover, our compounds P7 and P11 exhibited higher antiproliferative activity and selectivity against A549 and NCIH522 cells compared to the clinically approved drugs Afatinib and Gefitinib. The cell cycle analysis showed that the compound P7 and P11 arrests the cell cycle at G0/G1 phase, whereas the compounds P13 and P14 involved in G2/M phase arrest. The results from antiproliferative activity screening, cell cycle analysis and kinase profiling indicate that the suitably substituted 1,3-diarylpyrazolones exhibit high antiproliferative activity against non-small cell lung cancer cells.

Graphical Abstract

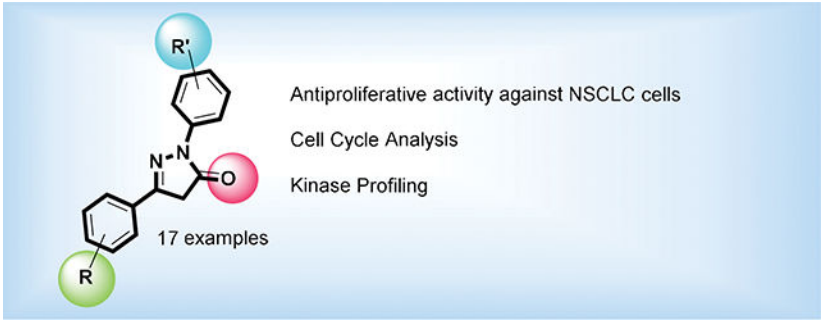

1,3-diarylpyrazolone compounds with halo-aryl moieties showed promising antiproliferative activities against non-small cell cancer cells, and the cell cycle analysis indicated that the di-halo-

Corresponding author murru@ulm.edu.

compounds arrest cell cycle at G2/M phase, whereas the mono-halo pyrazolone compound arrests at G0/G1 phase.

Keywords

Pyrazolones; Antiproliferative activty; NSCLC; Cell cycle analysis; Kinase Profiling

1. Introduction:

Despite immense advances in the field of basic and clinical research, cancer remains one of the leading causes of death in the world.[1] Moreover, lung cancer is the most common type of cancer with a morbidity rate of 11.6% and a mortality rate of 18.4% globally.[2] In the U.S., lung cancer is by far the leading cause of cancer-related death among both men and women; more deaths are caused by lung cancer every year than by breast, prostate, and colon cancer combined. Approximately 85% of lung cancers are within a group of histological subtypes collectively known as Non-Small Cell Lung Cancer (NSCLC), of which lung adenocarcinoma and lung squamous cell carcinoma are the most common.[3] Although the treatment with Tyrosine Kinase Inhibitors (TKIs) has improved the outcomes for patients with NSCLC, acquired resistance to TKIs causing the treatment failure and therefore new non-TKI therapeutics are desperately needed.[4]

Nitrogen heterocyclic compounds are an integral part of a huge number of natural and synthetic compounds and play important roles in the biological systems. Among various heterocyclic compounds, pyrazole and pyrazolone derivatives attracted huge attention in recent years as synthetic scaffolds in combinatorial and medicinal chemistry.[5] Moreover, the broad-spectrum of pharmacology properties about pyrazolone derivatives have been reported including anti-microbial, anti-oxidant, anti-inflammatory, anti-tubercular, anti-tumor, CNS activity, anti-viral, lipid-lowering, and antihyperglycemic activities.[6] For example, Edaravone (1) acts as an anti-ischemic neuroprotective agent, antipyrine and related drugs (2) act as analgesic, antipyretic, anti-inflammatory agents, 4,4'-dihalopyrazolone derivatives (3) act as human telomerase inhibitors and cytotoxic agents, Eltrombopag (4) acts as a drug for the treatment of idiopathic chronic immune thrombocytopenia, and other pyrazolone derivatives (5, 6, 7, 8 and 9) that exhibit anticancer properties related to breast, cervical and other cancers.[5,7] (Figure 1)

The high therapeutic properties of the pyrazolone compounds have encouraged organic chemists to synthesize many novel chemotherapeutic agents. Despite numerous studies reported on the biological activities of pyrazolone derivatives, most of the reports indicate the use of 1-aryl-3-alkylpyrazol-5-ones with various substitutions at the C4-position (**7**, Figure 2). Only a relatively small group of compounds contain 1-aryl-3-phenyl pyrazolones with the variations on rings '**A**' and '**B**' but not on '**C**' (**8**, Figure 2). It is surprising to see that a very little focus is given to 1,3-diarylpyrazol-5-ones with substitutions on ring **C** that does not have substitutions at the C-4 position on ring **B**.[5] Therefore, we were interested in synthesizing the less explored class of pyrazolone derivatives (**9**) and investigating their antiproliferative activity with the main goal of identifying potential anticancer agents.

Accordingly, we synthesized 17 pyrazolone derivatives and evaluated their antiproliferative activities against A549 and NCIH522 cancer cell lines.

2. Results and Discussion

2.1. Chemistry

The classical strategy employed for the synthesis of pyrazolone derivatives involves the cyclization of hydrazines and β-ketoesters by the modified Knorr pyrazole synthesis.[6b,8] These condensation reactions are generally performed in reflux conditions in the presence of either acids (e.g. acetic acid, *p*-Toluene sulfonic acid) or bases (e.g. piperidine or NaH) in the boiling ethanol/methanol solvent. Alternatively, reactions of substituted hydrazines with β-ketoamides, *N*-hydroxy-β-ketoamides, β-ketothioesters or acrylates have been developed.[9] Recently, metal catalyzed synthetic approaches for pyrazolone derivatives have also been developed.[10] However, many of the reported procedures seem to work well with alkyl substituted pyrazolones but not for the diarylpyrazolones. Besides that, only one report discussed the chemoselectivity issues in pyrazolone synthesis.[9f] Keeping in view the demerits of the conventional techniques, we implemented microwave-assisted method for the synthesis of 1,3-diarylpyrazol-5-one derivatives. Recent reports indicate that the microwave-assisted methods enable reaching high temperatures quickly and transiently while maintaining good control over the reaction conditions. They are often much faster, cleaner, and able to produce higher yields as compared to conventional heating procedures.[11] Previously, three independent groups[12] reported microwave assisted synthesis of pyrazolones of type **7** and **8** but not **9**, using domestic (multi-mode) microwave which has safety, fire hazard, and reproducibility issues. Moreover, the solvent-free methods are only useful for the liquid substrates and that limits the scope of the reaction.[12a]

Our single-mode microwave assisted synthetic approach involves the use of both liquids as well as solid substrates for the synthesis of 1,3-diarylpyrazolones. (Scheme 1) We have optimized reaction conditions such as the reaction temperature, time, and the solvent system for the reaction of ethyl benzoylacetate and phenyl hydrazine. Among all the solvents (ethanol, acetonitrile, water, glycerol, dichloromethane) tested, water and glycerol combination produced the desired pyrazolone (**P3**) in good yield (88%) with only trace amount of the corresponding ethoxy pyrazole (**P3'**). It is established that water can act as a strong acid and/or a strong base in high-temperature reactions, thus avoiding the use of mineral acids and bases which must be neutralized when the reaction is complete.[13]

With the optimized conditions in hand, a set of 1,3-disubstituted pyrazolones (P1-P11, table 1) were initially synthesized and evaluated for their antiproliferative activity. Based on the preliminary activity data, we have synthesized additional compounds (P12-P17) with different substitution patterns. For antiproliferative activity comparison, P1 and P2 are synthesized using alkyl β-ketoesters. Based on the mass analysis, we identified the product P1 as a hydroxylated pyrazolone with C-H oxidation on C-4 carbon. This type of aerial oxidation is recently reported.[14] Except the products P1 and P2, all products are 1,3-diarylpyrazolones (P3-P17) which are synthesized in good to excellent yields using aryl β-ketoesters and arylhydrazines. A set of aryl β- ketoesters with -nitro, -bromo, -fluoro, -methoxy, and -trifluoromethyl substituents at different positions on benzene ring were

chosen to produce the **C**-ring substituted pyrazolones. Along with the desired pyrazolones, considerable amount (up to 20%) of alkoxy pyrazole formation was observed for the reactions of halo-arylhydrazines (P4, P5, P13, P14 and P15).[9f] However, we successfully converted those product mixtures into single pyrazolone product via de-alkylation of alkoxy pyrazoles by treating with HBr in acetic acid.[15]

2.1.1. Characterization data of all the synthesized pyrazolones

4-hydroxy-4,5-dimethyl-2-phenyl-2,4-dihydro-3H-pyrazol-3-one (P1): [14] White crystals, MP: 105 °C. ^{1}H NMR (400 MHz, $CDCl_3$): δ 1.51 (s, 3H), 2.16 (s, 3H), 4.44 (brs, 1H), 7.17 (t, 1H, J = 7.8 Hz), 7.36 (t, 2H, J = 7.8 Hz), 7.82 (d, 2H, J = 7.8 Hz). ^{13}C NMR (100 MHz, $CDCl_3$): δ 12.7, 22.2, 77.4, 119.0, 125.5, 129.0, 137.6, 163.5, 174.8. FT-IR: 691, 772, 896, 1085, 1150, 1221, 1366, 1389, 1493, 1594, 1698, 2915, 3406 cm^{-1}. MP: 110 °C. HRMS (ESI) calcd for $C_{11}H_{13}N_2O_2$ ($M+H^+$), 205.0975; found, 205.0975.

2-phenyl-5-propyl-2,4-dihydro-3H-pyrazol-3-one (P2): [27] White crystals, MP: 109 °C. ^{1}H NMR (400 MHz, $CDCl_3$): δ 1.05 (t, 3H, J = 8.0 Hz), 1.70 (m, 2H), 2.49 (t, 2H, J = 8.0 Hz), 3.43 (s, 2H), 7.20 (t, 1H, J = 8.0 Hz), 7.41 (t, 2H, J = 8.0 Hz), 7.89 (d, 2H, J = 8.0 Hz). ^{13}C NMR (100 MHz, $CDCl_3$): δ 14.0, 20.2, 33.3, 41.9, 119.1, 125.2, 129.0, 138.3, 160.12, 170.8. FT-IR: 692, 756, 1407, 1498, 1610, 1715, 2815, 2962, 3109 cm^{-1}. HRMS (ESI) calcd for $C_{12}H_{15}N_2O$ ($M+H^+$), 203.1179; found, 203.1181.

2,5-diphenyl-2,4-dihydro-3H-pyrazol-3-one (P3): [28] White crystals, MP: 136 °C, ^{1}H NMR (400 MHz, $CDCl_3$): δ 3.79 (s, 2H), 7.21 (t, 1H, J = 8.0 Hz), 7.40–7.45 (m, 5H), 7.74–7.76 (m, 2H), 7.96 (d, 2H, J = 8.0 Hz). ^{13}C NMR (100 MHz, $CDCl_3$): δ 39.7, 119.2, 125.4, 126.1, 128.9, 129.0, 130.8, 138.2, 154.8, 170.3. FT-IR: 690, 756, 1118, 1331, 1458, 1496, 1595, 1716, 2952, 3063 cm^{-1}. HRMS (ESI) calcd for $C_{15}H_{13}N_2O$ ($M+H^+$), 237.1022; found, 237.1021.

2-(4-bromophenyl)-5-phenyl-2,4-dihydro-3H-pyrazol-3-one (P4): [29] White crystals, MP: 152 °C, ^{1}H NMR (400 MHz, $CDCl_3$): δ 3.81 (s, 2H), 7.48 (brs, 3H), 7.53 (d, 2H, J = 8.0 Hz), 7.75 (d, 2H, J = 4.0 Hz), 7.91 (d, 2H, J = 8.0 Hz). ^{13}C NMR (100 MHz, $CDCl_3$): δ 39.6, 118.1, 120.3, 126.0, 129.0, 130.6, 131.0, 131.9, 137.2, 155.0, 170.1. FT-IR: 690, 757, 1331, 1489, 1594, 1716, 2923, 3061 cm^{-1}. HRMS (ESI) calcd for $C_{15}H_{12}BrN_2O$ ($M+H^+$), 315.0128; found, 315.0130.

2-(4-chlorophenyl)-5-phenyl-2,4-dihydro-3H-pyrazol-3-one (P5): [30] White crystals, MP: 163 °C, ^{1}H NMR (400 MHz, $CDCl_3$): δ 3.83 (s, 2H), 7.39 (d, 2H, J = 8.0 Hz), 7.49 (brs, 3H), 7.76 (d, 2H, J = 4.0 Hz), 7.97 (d, 2H, J = 8.0 Hz). ^{13}C NMR (100 MHz, $CDCl_3$): δ 39.6, 120.0, 126.0, 128.9, 129.0, 130.3, 130.6, 130.9, 136.7, 154.9, 170.1. FT-IR: 689, 758, 828, 1092, 1331, 1492, 1593, 1716, 2917, 3058 cm^{-1}. HRMS (ESI) calcd for $C_{15}H_{12}ClN_2O$ ($M+H^+$), 271.0633; found, 271.0633.

5-(4-nitrophenyl)-2-phenyl-2,4-dihydro-3H-pyrazol-3-one (P6): [31] White crystals, MP: 188 °C, ^{1}H NMR (400 MHz, $CDCl_3$): δ 3.88 (s, 2H), 7.25 (t, 1H, J = 8.0 Hz), 7.44 (t, 2H, J = 8.0 Hz), 7.93 (d, 4H, J = 12.0 Hz), 8.31 (d, 2H, J = 12.0 Hz). ^{13}C NMR (100 MHz,

$CDCl_3$): δ 39.4, 119.3, 124.4, 126.0, 126.7, 129.1, 136.5, 137.7, 148.8, 152.2, 169.9. FT-IR: 692, 754, 854, 1109, 1344, 1520, 1597, 1723, 2911, 3047 cm^{-1}. HRMS (ESI) calcd for $C_{15}H_{12}N_3O_3$ ($M+H^+$), 282.0873; found, 282.0870.

5-(4-bromophenyl)-2-phenyl-2,4-dihydro-3H-pyrazol-3-one (P7): [31] White crystals, MP: 168 °C, ^1H NMR (400 MHz, $CDCl_3$): δ 3.81 (s, 2H), 7.20–7.25 (m, 1H), 7.42 (t, 2H, J = 8.0 Hz), 7.56–7.59 (m, 2H), 7.62–7.64 (m, 2H), 7.93 (d, 2H, J = 8.0 Hz). ^{13}C NMR (100 MHz, $CDCl_3$): δ 39.5, 119.2, 125.6, 127.5, 129.0, 129.8, 132.3, 138.0, 153.7, 170.1. FT-IR: 690, 762, 1189, 1330, 1496, 1595, 1710, 2947, 3061 cm^{-1}. HRMS (ESI) calcd for $C_{15}H_{12}BrN_2O$ ($M+H^+$), 315.0128; found, 315.0124.

5-(4-fluorophenyl)-2-phenyl-2,4-dihydro-3H-pyrazol-3-one (P8): [31] White crystals, MP: 192 °C. ^1H NMR (400 MHz, $CDCl_3$): δ 3.86 (s, 2H), 7.18 (t, 2H, J = 8.0 Hz), 7.25 (t, 1H, J = 8.0 Hz), 7.46 (t, 2H, J = 8.0 Hz), 7.78–7.81 (m, 2H), 7.98 (d, 2H, J = 4.0 Hz). ^{13}C NMR (100 MHz, $CDCl_3$): δ 39.9, 116.3, 116.4, 119.3, 123.3, 125.6, 128.2, 128.3, 129.1, 129.6, 138.2, 153.8, 163.4, 165.4, 170.3. FT-IR: 583, 692, 765, 1119, 1218, 1328, 1498, 1595, 1708, 2950, 3062 cm^{-1}. HRMS (ESI) calcd for $C_{15}H_{11}FN_2O$ ($M+H^+$), 255.0928; found, 255.0929.

5-(4-methoxyphenyl)-2-phenyl-2,4-dihydro-3H-pyrazol-3-one (P9): [31] White crystals, MP: 139 °C. ^1H NMR (400 MHz, $CDCl_3$): δ 3.84 (s, 2H), 3.89 (s, 3H), 6.99 (d, 2H, J = 8.0 Hz), 7.23 (t, 1H, J = 8.0 Hz), 7.45 (t, 2H, J = 8.0 Hz), 7.74 (d, 2H, J = 8.0 Hz), 8.00 (d, 2H, J = 8.0 Hz). ^{13}C NMR (100 MHz, $CDCl_3$): δ 39.9, 55.6, 114.5, 119.2, 123.8, 125.3, 127.8, 129.0, 138.4, 154.6, 161.8, 170.4. FT-IR: 754, 1167, 1248, 1466, 1559, 1715, 2838, 2949, 2061 cm^{-1}. HRMS (ESI) calcd for $C_{16}H_{15}N_2O_2$ ($M+H^+$), 267.1128; found, 267.1126.

5-(3-methoxyphenyl)-2-phenyl-2,4-dihydro-3H-pyrazol-3-one (P10): [32] White crystals, MP: 121 °C. ^1H NMR (400 MHz, $CDCl_3$): δ 3.73 (s, 2H), 3.79 (s, 3H), 6.91–6.93 (m, 1H), 7.14 (t, 1H, J = 8.0 Hz), 7.20 (d, 1H, J = 8.0 Hz), 7.26–7.30 (m, 2H), 7.35 (t, 2H, J = 8.0 Hz), 7.89 (d, 2H, J = 8.0 Hz). ^{13}C NMR (100 MHz, $CDCl_3$): δ 39.9, 55.6, 111.0, 116.8, 118.9, 119.3, 125.5, 129.1, 130.2, 132.3, 138.3, 154.7, 160.2, 170.4. FT-IR: 690, 757, 1040, 1168, 1253, 1321, 1468, 1562, 1507, 1717, 2836, 2950, 2063 cm^{-1}. HRMS (ESI) calcd for $C_{16}H_{15}N_2O_2$ ($M+H^+$), 267.1128; found, 267.1128.

2-phenyl-5-(4-(trifluoromethyl)phenyl)-2,4-dihydro-3H-pyrazol-3-one (P11): [31] White crystals, MP: 166 °C. ^1H NMR (400 MHz, $CDCl_3$): δ 3.80 (s, 2H), 7.17 (t, 1H, J = 8.0 Hz), 7.37 (t, 2H, J = 8.0 Hz), 7.65 (d, 2H, J = 4.0 Hz), 7.81 (d, 2H, J = 4.0Hz), 7.88 (d, 2H, J = 4.0 Hz). ^{13}C NMR (100 MHz, $CDCl_3$): δ 39.7, 119.4, 123.4, 125.8, 125.9, 126.2, 129.2, 129.6, 132.0, 132.3, 132.6, 132.8, 134.3, 138.1, 153.3, 170.1, 171.4. FT-IR: 691, 756, 831, 1069, 1127, 1168, 1322, 1596, 1713, 2958, 3046 cm^{-1}. HRMS (ESI) calcd for $C_{16}H_{12}F_3N_2O$ ($M+H^+$), 305.0896; found, 305.0894.

2-phenyl-5-(2,3,4,5-tetrafluorophenyl)-2,4-dihydro-3H-pyrazol-3-one (P12): Gum, ^1H NMR (400 MHz, $CDCl_3$): δ 3.90 (s, 2H), 7.23 (t, 1H, J = 8.0 Hz), 7.42 (t, 2H, J = 8.0 Hz), 7.69–7.71 (m, 1H) 7.89 (d, 2H, J = 8.0 Hz). ^{13}C NMR (100 MHz, $CDCl_3$): δ 41.9, 108.05, 108.08, 108.11, 108.26, 108.29, 108.32, 119.1, 122.3, 125.9, 129.1, 137.6, 147.9,

170.0. FT-IR: 691, 761, 828, 1009, 1078, 1121, 1343, 1432, 1477, 1531, 1593, 1723, 2952, 3056 cm^{-1}. HRMS (ESI) calcd for $C_{15}H_9F_4N_2O$ ($M+H^+$), 309.0646; found, 309.0644.

2-(4-bromophenyl)-5-(4-fluorophenyl)-2,4-dihydro-3H-pyrazol-3-one (P13): White crystals, MP: 197 °C. ^1H NMR (400 MHz, $CDCl_3$): δ 3.82 (s, 2H), 7.14 (t, 2H, J = 8.0 Hz), 7.52 (d, 2H, J = 8.0 Hz), 7.73–7.77 (m, 2H), 7.88 (d, 2H, J = 8.0 Hz). ^{13}C NMR (100 MHz, $CDCl_3$): δ 39.7, 116.2, 116.4, 118.3, 120.4, 124.5, 128.1, 128.2, 132.0, 132.6, 137.2, 153.99, 154.00, 163.1, 165.6, 170.0. FT-IR: 752, 824, 1011, 1126, 1322, 1593, 1706, 2939, 3048 cm^{-1}. HRMS (ESI) calcd for $C_{15}H_{11}BrFN_2O$ ($M+H^+$), 333.0033; found, 333.0034.

2,5-bis(4-bromophenyl)-2,4-dihydro-3H-pyrazol-3-one (P14): White crystals, MP: 183 °C. ^1H NMR (400 MHz, $CDCl_3$): δ 3.85 (s, 2H), 7.56 (d, 2H, J 8.0 Hz), 7.61–7.66 (m, 4H), 7.91 (d, 2H, J = 8.0 Hz). ^{13}C NMR (100 MHz, $CDCl_3$): δ 39.6, 118.5, 120.5, 125.6, 127.6, 129.7, 132.1, 132.4, 137.3, 154.1, 170.1. FT-IR: 499, 821, 1006, 1068, 1123, 1486, 1589, 1699, 2942, 3056 cm^{-1}. HRMS (ESI) calcd for $C_{15}H_{11}Br_2N_2O$ ($M+H^+$), 392.9233; found, 392.9234.

2-(4-bromophenyl)-5-(2-fluorophenyl)-2,4-dihydro-3H-pyrazol-3-one (P15): White crystals, MP: 151 °C. ^1H NMR (400 MHz, $CDCl_3$): δ 3.96 (s, 2H), 7.17 (t, 1H, J = 8.0 Hz), 7.27 (t, 1H, J = 8.0 Hz), 7.43–7.48 (m, 1H), 7.54 (d, 2H, J = 8.0 Hz), 7.91 (d, 2H, J = 8.0 Hz), 8.09 (t, 1H, J = 8.0 Hz). ^{13}C NMR (100 MHz, $CDCl_3$): δ 42.47, 42.55, 116.5, 116.7, 118.2, 120.3, 124.71, 124.75, 127.50, 127.62, 131.9, 132.5, 132.6, 137.1, 151.0, 159.6, 162.2, 170.44, 170.48. FT-IR: 759, 825, 1012, 1213, 1492, 1721 cm^{-1}. HRMS (ESI) calcd for $C_{15}H_{11}BrFN_2O$ ($M+H^+$), 333.0033; found, 333.0029.

1-(4-bromophenyl)-5-ethoxy-3-(2-fluorophenyl)-1H-pyrazole (P15'): Gummy liquid. ^1H NMR (400 MHz, $CDCl_3$): δ 1.48 (t, 3H, J = 8.0 Hz), 4.25 (q, 2H, J = 8.0 Hz), 6.16 (d, 1H, J = 4.0 Hz), 7.09–7.14 (m, 1H), 7.17–7.21 (m, 1H), 7.27–7.33 (m, 1H), 7.55 (d, 2H, J = 8.0 Hz), 7.74 (d, 2H, J = 8.0 Hz), 8.09–8.13 (m, 1H). ^{13}C NMR (100 MHz, $CDCl_3$): δ 14.7, 68.4, 87.44, 87.54, 116.03, 116.25, 119.7, 123.5, 124.39, 124.42, 128.27, 128.30, 129.70, 129.79, 132.0, 137.6, 145.7, 155.1, 159.1, 161.6, 171.3. GC-MS for C17H14BrFN2O, m/z = 361.2 (M+).

5-(4-bromophenyl)-2-(4-(trifluoromethyl)phenyl)-2,4-dihydro-3H-pyrazol-3-one (P16): White crystals, MP: 154 °C. ^1H NMR (400 MHz, $CDCl_3$): δ 3.84 (s, 2H), 7.62–7.65 (m, 2H), 7.67–7.69 (m, 2H), 7.70 (d, 2H, J = 8.0 Hz), 8.16 (d, 2H, J = 8.0 Hz). ^{13}C NMR (100 MHz, $CDCl_3$): δ 39.7, 118.6, 125.8, 126.3, 126.4, 127.7, 129.6, 132.5, 141.0, 154.4, 170.4, 171.4. FT-IR: 758, 820, 838, 1066, 1116, 1325, 1427, 1492, 1695, 2982 cm^{-1}. HRMS (ESI) calcd for $C_{16}H_{11}BrF_3N_2O$ ($M+H^+$), 383.0001; found, 383.0003.

5-(4-bromophenyl)-2-(3,5-dichlorophenyl)-2,4-dihydro-3H-pyrazol-3-one (P17): White crystals, MP: 194 °C. ^1H NMR (400 MHz, $CDCl_3$): δ 3.85 (s, 2H), 7.19 (brs, 1H), 7.62–7.63 (m, 4H), 7.99 (d, 2H, J = 8.0 Hz). ^{13}C NMR (100 MHz, $CDCl_3$): δ 39.5, 116.7, 125.0, 125.7, 127.5, 129.2, 132.3, 135.3, 139.5, 154.2, 169.8. FT-IR: 668, 727, 819, 867, 1066, 1174, 1311, 1429, 1583, 1701, 2958, 3042 cm^{-1}. HRMS (ESI) calcd for $C_{15}H_{10}BrCl_2N_2O$ ($M+H^+$), 382.9348; found, 382.9346.

2.2. Pharmacology

2.2.1. Antiproliferative activity—The antiproliferative activities of P1–P17, including P15', against two human lung adenocarcinoma cell lines (A549 and NCI-H522) were evaluated using CellTiter Glo assay.[16] All assays were performed in triplicates and the average of the cytotoxicity data, expressed as IC_{50} values, are summarized in Table 2. This table also compares the activity of Afatinib and Gefitinib, two clinically approved drugs to treat NSCLC.[17]. A549 cells are derived from epithelial carcinoma of non-small cell lung cancer patient with KRAS mutation and EGFR wild type[18] and NCI-H522 are also non-small cell lung cancer cell lines with *p53* gene mutation.[19] As mentioned above, our initial screening of compounds P1-P11 against A549 and NCI-H522 cells indicated that the presence of 1,3-diarylpyrazolone moiety is important for the antiproliferative activity. (Table 2) Accordingly, we have synthesized and evaluated the antiproliferative activity of another set of 1,3-diarylpyrazolone derivatives (P12-P17) with different substitutions on both rings A and C. All the 1,3-diarylpyrazolone derivatives displayed dose-dependent trends against A549 and NCI-H522 cells with IC_{50} values ranging from 1.98 μM to >100 μM. (Figures, SI)

Among all, the compounds bearing halogen substitutions on para-positions of A and/or C rings exhibited strong inhibitory effect against both cancer cell lines. However, pyrazolones with para- halo-substitutions on ring A (P4, P5) seems to be more cytotoxic when compared to the compounds bearing halogens at para-position of ring C (P7, P8), especially towards A549 and non-cancerous human lung fibroblast cells. This same trend is reflected with the para-disubstituted pyrazolones (P13, P14 and P16) that have -fluoro, -bromo and -trifluoromethyl groups. However, P7 exhibits high selectivity index as it is highly potent towards NCIH522 and A549 compared to non-cancerous HLF cells. Compounds P9 and P10 carries methoxy substituents on ring "C", that showed significantly less activity compared to parent compound P3 and the halo-substituted pyrazolone compounds. Even though less effective than parent pyrazolone P3, the compounds P6 (4-nitro, IC_{50} = 39.56 μM) and P9 (4-methoxy, IC_{50} = 42.25 μM) exhibits relatively high antiproliferative activity when compared to P10 (3-methoxy, IC_{50} >100 μM) which signifies the importance of para-substitution on ring **C**. In comparison to pyrazolone P15, the high IC_{50} values 51.09 μM (A549) and 61.70 μM (NCIH522) of alkoxypyrazole P15' indicates the required presence of amide carbonyl (C=O) in pyrazolones for exhibiting high antiproliferative activity. Most importantly, the pyrazolones P7 and P11 exhibited less cytotoxicity against non-cancerous lung fibroblast cells (IC_{50}: 61.26 μM and 26.06 μM) compared to A549 and NCIH522 lung cancer cells and therefore P7 and P11 can be tuned further to improve the potency while retaining or possibly improving the selectivity index. Moreover, compounds P7 and P11 outperformed both positive controls Afatinib and Gefitinib in terms of antiproliferative activity and selectivity. Additionally, it is possible to use the targeted drug delivery approach such as liposomal drug delivery strategy[20] for the highly potent compounds that have less selectivity index (P4, P5, P13-P16).

2.2.2. Cell Cycle Analysis—With the antiproliferative activity and structure activity relationship data in hand, we performed cell cycle analysis of selected pyrazolone compounds to gain preliminary insights on the mechanism of action. The antiproliferative activity trends against cancerous and non-cancerous cells indicates that the potency of

compounds results from either targeting DNA directly or indirectly. The cell cycle arrest is an important sign for inhibition of proliferation and the series of events that take place in a cell leading to its division and replication. Accordingly, we studied the effect of P7 and P11 on cell cycle progression in NCI-H522 cells using flow cytometry. Treatment of NCI-H522 cells with P7 and P11 for 48hrs at 5 μM concentration resulted in more cell population in G0/G1 phase with a corresponding decrease of cell percentage in both S and G2/M phases as shown in Figure 3. A recent report by Zhu et al. indicated that a similar nitrogen heterocyclic compound, dihydropyrrolone, acts as a potent G0/G1-phase arresting agent inducing cell apoptosis by regulating the levels of p53 and p21/cyclin D1.[21]

In addition to P7 and P11, we studied the effect of other potent pyrazolones P13 and P14 on the cell cycle progression. Interestingly, the treatment of NCI-H522 cells with P13 and P14 for 48hrs at 5 μM concentration resulted in more cell population in G2/M phase with a corresponding decrease of cell percentage in both G1 and S phases. (Figure 4) It is indicative that para-halo substituted pyrazolones could influence NCI-H522 cell cycle progression at low micromolar concentration.

Recently, Camero et. al. reported that pretreatment with three poly (ADP-ribose) polymerase-1 (PARP1) inhibitors (Olaparib, Iniparib, Veliparib) was able to sensitize soft tissue sarcoma cells to radiation by inducing cell cycle arrest at the G2/M checkpoint.[22] In general, cancer cells are more reliant on the G2/M checkpoint for DNA repair than non-cancerous cells due to G1/S DNA repair deficiencies, and therefore halting cell cycle progression through the G2/M checkpoint selectively induces apoptosis in cancer cells. The cell cycle analysis results confirmed that the pyrazolone P7 influences NCI-H522 cell cycle progression in a different way than P13 and P14 (G0/G1 Vs G2/M) which partly explains the difference in their selectivity towards non-cancerous cells. As most kinases responsible for the cell cycle regulation and anti-apoptotic activity,[23] the kinase inhibition activity of compound P7 was tested across the kinome to get information on target selection. Among the various biological targets for pyrazole derivatives, kinases are those of choice as the presence of the extra nitrogen atom increases the possible fits in the ATP active site which requires well positioned H bond donor acceptor systems.

2.2.3. Kinase Activity Profiling—Under the current drug discovery process, ‘high-throughput kinase profiling’ has become the standard approach for the discovery of lead compounds for established as well as unexplored kinase targets.[24] Literature also reveals that many of the previously reported pyrazolone-based antitumor agents inhibit different kinases such as VEGFR-2, ALK, c-Met.[25] As part of our mechanistic investigation of antiproliferative activity, compound P7 was screened over a panel of 485 kinases (including 110 oncogenic kinases) using outsourced Kinase Profiling Service.[24b] Surprisingly, compound P7 showed no potential inhibitory activity against any tested kinase, except for the modest activity against ACVRL1 (47%), ANKK1(50%) and NUAK2(41%) kinases. These results indicate that the mechanism of action of pyrazolone P7 is perhaps different from other previously reported pyrazolones.[5a,25]

3. Conclusions

We have developed a microwave assisted synthetic approach for the synthesis of 1,3-diarylpyrazolone compounds. All the synthesized compounds have been characterized by FT-IR, GC-MS, HR-MS and NMR spectroscopy and evaluated their antiproliferative activities against two non-small cell lung cancer cell lines namely A549 and NCIH522. A set of pyrazolone compounds displayed high inhibitory potential with low IC_{50} values against both cancer and non-cancerous cells. However, the pyrazolones P7 and P11 exhibited promising antiproliferative activity against cancer cell lines while being less cytotoxic to non-cancerous human lung fibroblast cells. Cell cycle analysis and kinase profiling assays were performed to gain additional insights on the mechanism of action. The cell cycle analysis indicated that the compounds P13 and P14 arrest cell cycle at G2/M phase in NCIH522 cells, whereas pyrazolone P7 and P11 arrest cell cycle at G0/G1 phase indicating the possible differences in their mechanism of action. Additionally, the kinase inhibitory activities of pyrazolone P7 was tested against a panel of 485 kinases, including 110 oncogenic kinases. Unlike many other nitrogen heterocyclic compounds, P7 did not exhibit considerable inhibition of any cancer related kinases. Overall, the results indicated that the suitably substituted 1,3-diarylpyrazolone compounds are highly potent against non-small cell lung cancer cells and the pyrazolone P7 can be tuned further to develop selective and potent non-kinase inhibitors with promising anticancer activity. While this initial chemistry and pharmacology effort has produced interesting pyrazolone analogs, we continue to seek compounds that are more potent and have improved ADME properties (i.e., lower IC_{50}, improved metabolic stability, longer half-life) through structure-based design.

4. Materials and methods:

4.1. Chemistry

4.1.1. General information: For the chemistry portion of this study, all solvents and other chemicals were obtained/purchased from Sigma-Aldrich, and TCI. All the reagents were commercial grade and if applicable, the solvents were purified according to the established procedures, or were used without further purification. Organic extracts were dried over anhydrous sodium sulfate. After completion of the reactions, solvents were removed on a rotary evaporator under reduced pressure using Buchi Rotavapor equipped with a vacuum controller and vacuum pump. Silica gel (60–120 mesh size) was used for column chromatography. Reactions were monitored by TLC on silica gel precoated aluminum cards with fluorescent indicator visualizable at 254 nm (0.25mm). Developed plates were visualized using a Spectroline ENF 260C/FE UV apparatus. NMR spectra were recorded on JEOL 400 MHz FT spectrometer in $CDCl_3$ solvent. Chemical shifts are expressed in δ units (ppm) from tetramethylsilane (TMS) used as the internal standard for ^{1}H NMR (400 MHz) and for ^{13}C NMR (100 MHz). Infrared spectra (IR) were run on a SpectrumOne FT-IR spectrophotometer. Band position and absorption ranges are given in cm^{-1}. GC-MS analysis carried out on an Agilent GC-MS (7890A – 5975C VL MSD) system. High Resolution Mass Spectrometry (HRMS) was performed on an Agilent 6230, and spectra recorded by electro-spray ionization (ESI) with a Q-TOF. Microwave-assisted reactions were performed on Discover S-Class (CEM) single mode

microwave reactor with the instrument settings controlled by using PC-running Synergy 1.4 software. All experiments were carried out in microwave reaction vials using a stirring bar. Stirring, temperature, irradiation power, PowerMAX (in situ cooling during the microwave irradiation), ramp and hold times were set as indicated. Temperature of the reaction was monitored by a built-in infrared sensor. After completion of the reaction, the mixture was cooled to 25 °C via air-jet cooling.

4.1.2. General Procedures for the Microwave Assisted Synthesis of 1,3-Diarylpyrazol-5-ones:

A 10 mL microwave reaction vial, equipped with a stir bar, charged with the substituted β-ketoester (2 mmol), the appropriate arylhydrazine (2 mmol), glycerol (1 mL) and water (1 mL). Then, the vial was sealed with Teflon-lined silicone cap and placed in the microwave reactor. Microwave irradiation of 300W was used and the temperature ramped from room temperature to 100 °C which takes about 1 minute. The reaction continued for 20 minutes at the same temperature while stirring. After that, the reaction mixture was cooled to room temperature, extracted with ethyl acetate, dried with sodium sulfate, and solvent was removed under vacuum to get the crude product. If the crude product is solid, it was recrystallized using acetonitrile solvent to obtain pure product in crystalline form. In some cases, the products were purified by column chromatography using hexane-ethyl acetate as eluent.

4.1.3. Structures assignment: GC-MS, FT-IR, ESI-MS (HRMS), ^{1}H- and ^{13}C-NMR analysis—

The structures of all the synthesized pyrazolone derivatives were confirmed by ^{1}H-NMR, ^{13}C-NMR, FT-IR, GC-MS and HRMS analysis. Compounds P1-P11 reported earlier and the P12-P17 are new compounds. Based on the literature, *N*-substituted pyrazol-5-ones exists in the tautomeric forms as shown below.[26] The research indicates that the form which will be more dominant depends mainly on the type of solvent it is dissolved in. In the gaseous phase, apolar solvent and solvents with low polarity, such as CH_2Cl_2, $CHCl_3$, and CCl_4, only the keto form is observed. The enol form is predominant in polar solvents, such as DMSO, THF, and CH_3CN. NMR of all our compounds in $CDCl_3$ show a clear -CH_2- signal in the pyrazolone ring and the absence of a broad peak around 10–12 ppm in ^{1}H-NMR confirms the absence of enol (OH proton) form. Single-crystal X-ray crystallography analysis of **P13** confirms the same. (Figure 5)

4.2. Pharmacology

4.2.1. Antibodies, Chemicals and Reagents—

CellTiter Glo® reagent (Catalog # G9242) for anti-proliferative assay was purchased from Promega Corporation (Madison, WI). Celecoxib as a positive control for anti-proliferative activity was purchased from TCI America. Propidium Iodide flow cytometry kit (Catalog # ab139418) for cell cycle analysis was purchased from Abcam (Cambridge, MA).

4.2.2. Cell lines and culture—

A549 and NCI-H522 are non-small cell lung adenocarcinoma cell lines and were purchased from American Type Culture Collection (ATCC, Rockville, MD). Both cell lines were cultured in RPMI 1640 (ATCC) with 10% (v/v) FBS, 0.01 mg/mL bovine insulin and 0.1 mg/mL penicillin/streptomycin. Primary Lung Fibroblast, Non-cancerous, Human (HLF) cell line was purchased from ATCC and

was cultured in fibroblast basal medium supplemented with fibroblast growth kit-low serum components (ATCC). All the cells were maintained at 37 °C with 5% CO_2. The cells were passaged two to three times before conducting all the experiments.

4.2.3. Evaluation of Antiproliferative Activity by Cell-Titer Glo assay—

Determination of anti-proliferative activity of the compounds was carried out using a Cell Titer-Glo® Luminescent cell viability assay (Promega Corporation, Madison, WI). In this assay, cell viability is determined and analyzed by the quantitation of ATP in the cells as the number of ATP present is proportional to number of viable cells. This cell-based assay was done in 96-well plate in which approximately 10,000 cells per well were coated using the complete medium and incubated overnight at 37°C and 5% CO_2.Various concentrations of the compounds were prepared by dilution with serum-free medium and triplicates of each concentration were used for treatment. A wide range of concentration of compounds from 0.001 to 100 μM (100 μL/well) were used. 0.2% sodium dodecyl sulfate (SDS) and 1% dimethyl sulfoxide (DMSO) treated cells were used as negative and positive controls, respectively. The treated cells were incubated for 72 hours at 37°C and 5% CO_2. After the incubation, the cells were washed with phosphate buffer saline (PBS) and 100 μL/well of CellTitre-Glo® reagent was added. Then, they were further incubated for 20 mins and their luminescence was measured using microplate luminescence analyzer (Biotek Synergy, Winooski, VT, USA). IC_{50} was determined by plotting a log dose-response curve using Prism® (GraphPad software, La Jolla, CA).

4.2.4. Cell Cycle Analysis—Approximately 1×10^5 NCI-H522 cells were seeded onto 6 well-plate overnight and then treated with 5 μM of P7, P11, P13 and P14 in serum-free medium for 48 hours. After incubation, the cells were washed with PBS and then fixed with 70% ethanol for 2hours at −20 °C dropwise with intermittent vortexing. After centrifuging at high speed (10000 rpm) for 5 min, the supernatant was aspirated, and the cells were then washed twice with PBS. Washed cells were resuspended in distilled water with 100 μg/mL RNase and 40 μg/mL propidium iodide, followed by incubation at 37°C for 30 minutes. After washing with PBS, the cells were analyzed for DNA content (10,000) using a FACSCalibur flow cytometry instrument (BD Biosciences, San Jose, CA) operated with CellQuest Pro software (BD Biosciences). Appropriate FSC vs SSC gate was conducted during the flow cytometric analysis to remove the cell debris and cell aggregates. The experiments were repeated in triplicate and those without compound treatment were taken as control.

4.2.5. Kinase Activity Profiling—ThermoFisher (SelectScreen Kinase Profiling) used FRET assays based on the differential sensitivity of phosphorylated and non-phosphorylated peptides to proteolytic cleavage and employs a fluorescence-based, coupled-enzyme format. The peptide substrate is labeled with two fluorophores-one at each end-that make up a FRET pair. The kinases that are inhibited at >80% will then be chosen for further dose-response curve determination by the 10-point 4-log IC_{50} determinations.

Supplementary Material

Refer to Web version on PubMed Central for supplementary material.

Acknowledgements

This work was supported by LBRN Full Award (to SM) from an Institutional Development Award (IDeA) #P2OGM103424–20, received from the National Institute of General Medical Sciences of the National Institutes of Health (NIGMS/NIH) and the RCS Grant#LEQSF-RD-A-35 (to SM) from Louisiana Board of Regents.

6. Bibliography

1. a)Wong MCS, Lao XQ, Ho K-F, Goggins WB, Tse SLA, Incidence and mortality of lung cancer: global trends and association with socioeconomic status, Sci. Rep. 7 (2017), pp 14300, 1–9. [PubMed: 29085026] b) http://www.cancer.org/research/cancerfactsstatistics/
2. Bray F, Ferlay J, Soerjomataram I, Siegel RL, Torre LA, Jemal A, Global cancer statistics 2018: GLOBOCAN estimates of incidence and mortality worldwide for 36 cancers in 185 countries CA Cancer J. Clin, 68 (2018), pp. 394–424. [PubMed: 30207593]
3. Travis WD, Brambilla E, Nicholson AG, et al. The 2015 World Health Organization classification of lung tumors: impact of genetic, clinical and radiologic advances since the 2004 classification, J. Thorac. Oncol, 10 (2015), pp. 1243–1260. [PubMed: 26291008]
4. a)Rosenzweig SA Acquired resistance to drugs targeting tyrosine kinases, Adv. Cancer Res. 138 (2018), pp. 71–98. [PubMed: 29551130] b)Lovely CM, Combating acquired resistance to tyrosine kinase inhibitors in lung cancer, Am. Soc. Clin. Oncol. Educ. Book (2015) e165–73. [PubMed: 25993168]
5. a)Zefeng Z, Xufen D, Chenyang L, Xiao W, Jiale T, Ying F, Jing X, Cong M, Zhuang N, Peinan F, Mingcheng Q, Xirui H, Shaoping W, Yongmin Z, Xiaohui Z, Pyrazolone structural motif in medicinal chemistry: Retrospect and prospect, Eur. J. Med. Chem. 186 (2020), 111893. [PubMed: 31761383] b)Kucukguzel SG, Senkardes S, Recent advances in bioactive pyrazoles, Eur. J. Med. Chem. 97 (2015), pp. 786–815. [PubMed: 25555743] c)Bailly C, Potential use of edaravone to reduce specific side effects of chemo-, radio- and immuno-therapy of cancers, Int. Immunopharmacol. 77 (2019), 105967. [PubMed: 31670091]
6. a)Vijesh AM, Isloor AM, Isloor S, Shivananda KN, Shyma PC, Arulmoli T, Synthesis of some new pyrazolone derivatives as potent antimicrobial agents, Der Pharma Chemica, 3 (2011), pp. 454–463.b)Venkat RR, Vijayakumar V, Suchetha KN, Synthesis of some novel bioactive 4-oxy/thio substituted-1H-pyrazol-5(4H)-ones via efficient cross-Claisen condensation, Eur. J. Med. Chem. 44 (2009), pp. 3852–3857. [PubMed: 19423195] c)Soni JP, Sen DJ, Modh KM, Structure activity relationship studies of synthesised pyrazolone derivatives of imidazole, benzimidazole and benztriazole moiety for anti-inflammatory activity, J. Appl. Pharm. Sci, 1 (2011), 115–120.d)Passi NA, Prajapati MK, Sen DJ, Anand IS, Pharmacological study of biotransformation of substituted and unsubstituted indanone acetic acid adduct with pyrazolone ring for analgesic activity in-vivo, Int. J. Drug Dev. & Res 2 (2010), pp. 182–189.e)Fahmy HH, Khalifa NM, Nossier ES, Abdalla MM, Ismail MMF, Synthesis and anti-inflammatory evaluation of new substituted 1-(3-chlorophenyl)-3-(4-methoxyphenyl)-1H-pyrazole derivatives, Acta Pol. Pharm. Drug Res 69 (2012), pp. 411–421.f)Ailawadi S, Jyoti YM, Pathak D, Synthesis and characterization of some substituted pyrazoles as analgesics and anti-inflammatory agents, Der Pharma Chemica, 3 (2011), pp. 215–222.g)Gunasekaran P, Perumal S, Yogeeswari P, Sriram D, A facile four-component sequential protocol in the expedient synthesis of novel 2-aryl-5-methyl-2,3-dihydro-1H-3-pyrazolones in water and their antitubercular evaluation, Eur. J. Med. Chem. 46 (2011), pp. 4530–4536. [PubMed: 21839549] h)Bennani FE, Doudach L, Cherrah Y, Ramli Y, Karrouchi K, Ansar M, Faouzi MEA, Overview of recent developments of pyrazole derivatives as an anticancer agent in different cell line, Bioorg. Chem. 97 (2020), 103470. [PubMed: 32120072]
7. a)Nakagawa H, Ohyama R, Kimata A, Suzuki T, Miyata N, Hydroxyl radical scavenging by edaravone derivatives: Efficient scavenging by 3-methyl-1-(pyridin-2-yl)-5-pyrazolone with an intramolecular base, Bioorg. Med. Chem. Lett. 16 (2006), 5939–5942. [PubMed: 16997555] b)Freitag FG, Cady R, DiSerio F, Elkind A, Gallagher RM, Goldstein J, Klapper JA, Rapoport AM, Sadowsky C, Saper JR, Smith TR, Comparative study of a combination of isometheptene mucate, dichloralphenazone with acetaminophen and sumatriptan succinate in the treatment of migraine, Headache 41 (2001), pp. 391–398. [PubMed: 11318886] c)Himly M, Jahn-Schmid B, Pittertschatscher K, Bohle B, Grubmayr K, Ferreira F, Ebner H, Ebner C, IgE-mediated immediate-

type hypersensitivity to the pyrazolone drug propyphenazone, J. Allergy Clin. Immunol. 111 (2003), pp. 882–888. [PubMed: 12704373] d)Jing L, Wang L, Zhao Y, Tan R, Xing X, Liu T, Huang W, Luo Y, Li Z, Synthesis, Crystal Structure and Evaluation of Cancer Inhibitory Activity of 4-[indol-3-yl-Methylene]-1H-pyrazol-5(4H)-one derivatives, J. Chem. Res. 36 (2012), pp. 691–696.e)Bussel JB, Cheng G, Saleh MN, Psaila B, Kovaleva L, Meddeb B, Kloczko J, Hassani H, Mayer B, Stone NL, Arning M, Provan D, Jenkins JM, N. Eltrombopag for the Treatment of Chronic Idiopathic Thrombocytopenic Purpura, Engl. J. Med 357 (2007), pp. 2237–2247.

8. Stanovnik B, Svete J, In Science of Synthesis, Vol. 12; Neier R, Ed.; Georg Thieme Verlag; Stuttgart, New York, 2002, 15–225.
9. a)Abbady MS, Youssef MSK, Synthesis and biological activity of some new pyridines, pyrans, and indazoles containing pyrazolone moiety, Med. Chem. Res. 23 (2014), pp. 3558–3568.b)Tabei K, Kawashima E, Kato T, Reaction of N-Hydroxyacetoacetanilide with Carbonyl Reagents, Chem. Pharm. Bull. 29 (1981), 244–249.c)Wall M, Subasinghe N, Sui Z, Flores C, Substituted pyrazoles as n-type calcium channel blockers, PCT Int. Appl 2014. WO 2014028803A1.d)Eller GA, Holzer WM, A one-step synthesis of pyrazolone, Molbank, M464 (2006), 1–3.e)Duffy J, Darcy MG, Delorme E, Dillon SB, Eppley DF, Miller CE, Giampa L, Hopson CB, Huang Y, Keenan RM, Lamb P, Leong L, Liu N, Miller SG, Price AT, Rosen J, Shaw TN, Smith H, Stark KC, Tain SS, Tyree C, Wiggall KJ, Zhang L, Luengo JI, Hydrazinonaphthalene and Azonaphthalene Thrombopoietin Mimics Are Nonpeptidyl Promoters of Megakaryocytopoiesis, J. Med. Chem 44 (2001), pp. 3730–3745. [PubMed: 11606138] f)Štefane B, Polanc S, Aminolysis of 2,2-difluoro-4-alkoxy-1,3,2-dioxaborinanes: route to β-keto amides and β-enamino carboxamides, Tetrahedron, 63 (2007), pp. 10902.
10. a)Capua M, Granito C, Perrone S, Salomone A, Troisi L, Palladium-catalyzed carbonylative coupling of α-chloroketones with hydrazines: a simple route to pyrazolone derivatives, Tetrahedron Lett, 57 (2016), pp. 3363.c)Zhu Y-F, Wei B-L, Wei J-J, Wang W-Q, Song W-B, Xuan L-J, Synthesis of pyrazolones and pyrazoles via Pd-catalyzed aerobic oxidative dehydrogenation, Tetrahedron Lett. 60 (2019), pp. 1202–1205.
11. a)Alcazar J, Oehlrich D, Recent applications of microwave irradiation to medicinal chemistry, Future Med. Chem 2 (2010), 169–176. [PubMed: 21426184] b)Jiang B, Sh F, Tu SJ Microwave-Assisted Multicomponent Reactions in the Heterocyclic Chemistry, Curr. Org. Chem. 14 (2010), pp. 357–378.
12. a)Mojtahedi MM, Jalali MR, Abaee MS, Bolourtchian M, Microwave-assisted synthesis of substituted pyrazolones under solvent-free conditions, Heterocycl. Commun. 12 (2006), 225–228.b)Ma R, Zhu J, Liu J, Chen L, Shen X, Jiang H, Li J, Microwave-assisted one-pot synthesis of pyrazolone derivatives under solvent-free conditions, Molecules 15 (2010), 3593–3601. [PubMed: 20657501] c)Sivakumar KK, Rajasekaran A, Senthilkumar P, Wattamwar PP, Conventional and microwave assisted synthesis of pyrazolone Mannich bases possessing anti-inflammatory, analgesic, ulcerogenic effect and antimicrobial properties, Bioorg. Med. Chem. Lett. 24 (2014), pp. 2940–2944. [PubMed: 24835630]
13. de la Hoz A, Diaz-Ortiz A, Prieto P, CHAPTER 1: Microwave-Assisted Green Organic Synthesis, in Alternative Energy Sources for Green Chemistry, 2016, pp. 1–33.
14. Sheng X, Zhang J, Yang H, Jiang G, Tunable Aerobic Oxidative Hydroxylation/Dehydrogenative Homocoupling of Pyrazol-5-ones under Transition-Metal-Free Conditions. Org. Lett. 19 (2017), pp. 2618–2621. [PubMed: 28470068]
15. a)Zou CL, Ji H, Xie GB, Chen DL, Wang FP, An effective O-demethylation of some C19-diterpenoid alkaloids with HBr–glacial acetic acid, J. Asian Nat. Prod. Res. 10 (2008), pp. 1063–1067. [PubMed: 19031247] b)Delhaye L, Diker K, Donck T, Merschaert A, An organic solvent free process for the demethylation of 4-(4-methoxyphenyl)butanoic acid, Green Chem. 8 (2006), 181–182. c) We treated the reaction mixture with 30% HBr in acetic acid as shown below.

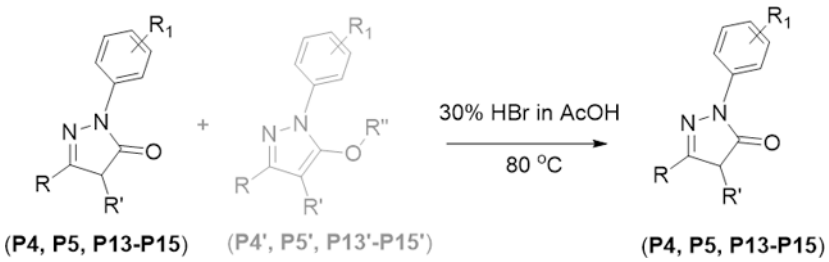

(**P4, P5, P13-P15**) (P4', P5', P13'-P15') (**P4, P5, P13-P15**)

16. Tolliday N, High-throughput assessment of Mammalian cell viability by determination of adenosine triphosphate levels, Curr. Protoc. Chem. Biol 2 (2010), 3, pp. 153–161.

17. a)Keating GM Afatinib: A Review in Advanced Non-Small Cell Lung Cancer. Target Oncol. 11 (2016), pp. 825–835. [PubMed: 27873136] b)Birnbaum A, Ready N Gefitinib therapy for non-small cell lung cancer. Curr. Treat Options Oncol. 6, (2005), pp. 75–81. [PubMed: 15610717]

18. Muralidharan R, Babu A, Amreddy N, Srivastava A, Chen A, Zhao YD, Kompella UB, Munshi A, Ramesh R Tumor-targeted Nanoparticle Delivery of HuR siRNA Inhibits Lung Tumor Growth In Vitro and In Vivo By Disrupting the Oncogenic Activity of the RNA-binding Protein HuR,Mol Cancer Ther. 16 (2017), 8, pp. 1470–1486. [PubMed: 28572169]

19. You L, Yang CT, Jablons DM ONYX-015 works synergistically with chemotherapy in lung cancer cell lines and primary cultures freshly made from lung cancer patients, Cancer Res. 60 (2000), 4, pp. 1009–13.

20. a)Yan W, Leung SSY, To KKW, Updates on the use of liposomes for active tumor targeting in cancer therapy, Nanomedicine 15 (2020), 3, pp. 303–318. [PubMed: 31802702] b)Krajewska JB, Bartoszek A, Fichna J New Trends in Liposome-based Drug Delivery in Colorectal Cancer, Mini Rev Med Chem 19 (2019), 1, pp. 3–11. [PubMed: 30179131]

21. a)Yang D, Huang C, Liao H, Zhang H, Wu S, Zhu Q, Zhou Z-Z, Discovery of Dihydropyrrol-2-ones as Novel G0/G1-Phase Arresting Agents Inducing Apoptosis, ACS Omega, 4 (2019), pp. 17556–17560. [PubMed: 31656929]

22. Camero S, Ceccarelli S, De Felice F, Marampon F, Mannarino O, Camicia L, et al. PARP inhibitors affect growth, survival and radiation susceptibility of human alveolar and embryonal rhabdomyosarcoma cell lines, J Cancer Res Clin Oncol. 145 (2019), pp. 137–52. [PubMed: 30357520]

23. Sielecki TM, Boylan JF, Benfield PA, Trainor GL, Cyclin-dependent kinase inhibitors: useful targets in cell cycle regulation, J. Med. Chem. 43 (2000), 1–18.

24. a)Watson NA, Cartwright TN, Lawless C, et al. Kinase inhibition profiles as a tool to identify kinases for specific phosphorylation sites, Nat. Commun. 11 (2020), 1684. [PubMed: 32245944] b)Miduturu CV, Deng X, Kwiatkowski N, Yang W, Brault L, Filippakopoulos P, Chung E, Yang Q, Schwaller J, Knapp S, King RW, Lee JD, Herrgard S, Zarrinkar P, Gray NS, High-Throughput Kinase Profiling: A More Efficient Approach toward the Discovery of New Kinase Inhibitors, Chem. Biol. 18 (2011), pp. 868–879. [PubMed: 21802008]

25. a)Tripathy R, Mchugh RJ, Ghose AK, Ott GR, Angeles TS, Albom MS, Zeck H, Aimone LD, Mangeng C, Dorsey BD, Pyrazolone-based anaplastic lymphoma kinase (ALK) inhibitors: Control of selectivity by a benzyloxy group, Bioorg. Med. Chem. Lett. 21 (2011), pp. 7261–7264. [PubMed: 22061645] b)Gu W, Dai Y, Hao Q, Wei S, Chen L, Zhao F, Huang W, Hai Q, Discovery of novel 2-substituted-4-(2-fluorophenoxy) pyridine derivatives possessing pyrazolone and triazole moieties as dual c-Met/VEGFR-2 receptor tyrosine kinase inhibitors, Bioorg. Chem. 72 (2017), pp. 116–122. [PubMed: 28411406] c)Norman MH, Longbin L, Matthew L, Ning X, Ingrid F, D'Angelo ND, Celia D, Karen R, Bellon SF, Tae-Seong K, Structure-Based Design of Novel Class II c-Met Inhibitors: 2. SAR and Kinase Selectivity Profiles of the Pyrazolone Series, J. Med. Chem. 55 (2012), pp. 1858–1867. [PubMed: 22320343] d)Longbin L, Norman MH, Matthew L, Ning X, Aaron S, Boezio AA, Shon B, Debbie C, D'Angelo ND, Julie G, Structure-Based Design of Novel Class II c-Met Inhibitors: 2. SAR and Kinase Selectivity Profiles of the Pyrazolone Series, J. Med. Chem. 55 (2012), pp. 1868–1897. [PubMed: 22320327]

26. Chmutova GA, Kataeva ON, Ahlbrecht H, Kurbangalieva AR, Movchan AI, Lenstra ATH, Geise HJ, Litvinov IA, Derivatives of 1-phenyl-3-methylpyrazol-2-in-5-thione and their oxygen

analogues in the crystalline phase and their tautomeric transformations in solutions and in the gas phase, J. Mol. Struct. 570 (2001), pp. 215–223.

27. Toonchue S, Sumunnee L, Phomphrai K, Yotphan S, Metal-free direct oxidative C–C bond coupling of pyrazolones and quinoxalinones. Org. Chem. Front 5 (2018), pp. 1928–1932.
28. LeBlanc A, Cuperlovic-Culf M, Morin PJ, Touaibia M, Structurally related edaravone analogues: synthesis, antiradical, antioxidant, and copper-chelating properties CNS Neurol Disord Drug Targets, 18 (2019), pp. 779–790. [PubMed: 31724516]
29. Shen S-J, Du X-L, Xu X-L, Wu Y-H, Zhao M-G and Liang J-Y, Regioselective *N*-Addition/Substitution Reaction of α-Alkylidene Pyrazolinones with Propargyl Sulfonium Salts to Construct Allylthio-Containing Pyrazolones, J. Org. Chem. 84 (2019), pp. 12520–12531. [PubMed: 31496249]
30. Li C, Liu Y, Wu S, Han G, Tu J, Dong G, Liu N, Sheng C, Targeting fungal virulence factor by small molecules: Structure-based discovery of novel secreted aspartic protease 2 (SAP2) inhibitors. Eur. J. Med. Chem. 201 (2020), 112515. [PubMed: 32623209]
31. Majed H, Johnston T, Kelso C, Monachino E, Jergic S, Dixon NE, Mylonakis E, Kelso MJ Structure-activity relationships of pyrazole-4-carbodithioates as antibacterials against methicillin–resistant Staphylococcus aureus, Bioorg. Med. Chem. Lett, 28 (2018), pp. 3526–3528. [PubMed: 30297281]
32. Desroses M, Jacques-Cordonnier M-C, Llona-Minguez S, Jacques S, Koolmeister T, Helleday T and Scobie M, A Convenient Microwave-Assisted Propylphosphonic Anhydride (T3P®) Mediated One-Pot Pyrazolone Synthesis, Eur. J. Org. Chem. 26 (2013), pp. 5879–5885.

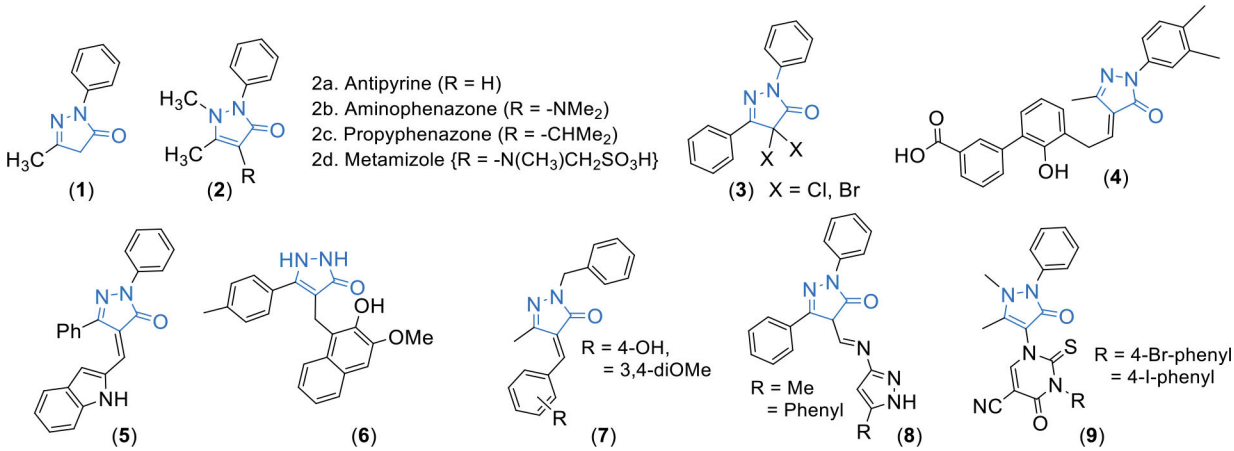

Figure 1.
Structures of biologically active pyrazolone derivatives

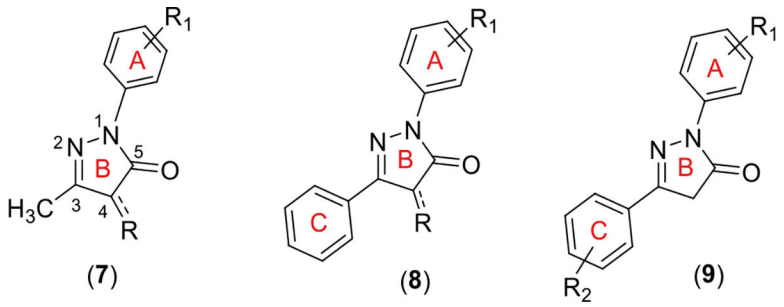

Figure 2.
General structures of pyrazolone derivatives with different substitution patterns

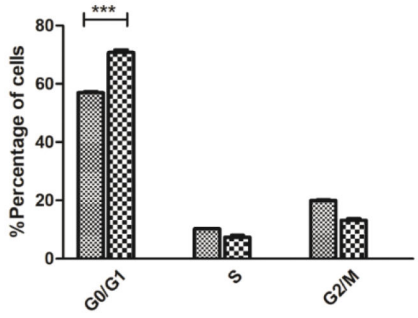

	Control	Treatment – P7
G0/G1	56.93 ±0.53	70.78±1.28
S	10.27 ±0.14	7.73±0.88
G2/M	19.96 ±0.41	13.17±0.87

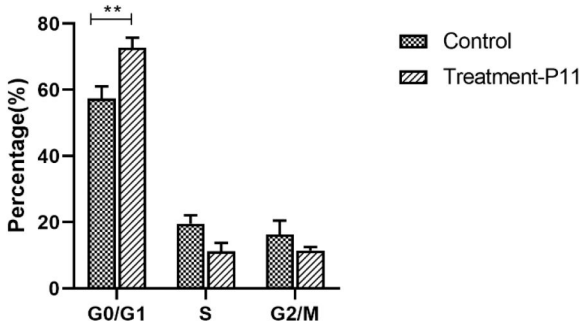

	Control	Treatment-P 11
G0/G1	57.4 ± 3.60	72.73 ± 3.01
S	19.56 ± 2.53	11.23 ± 2.52
G2/M	16.3 ± 4.21	11.4 ± 1.10

Figure 3.

Effects of pyrazolones **P7** and **P11** on the cell cycle progression of NCI-H522 cells, *** represents p-value < 0.001.

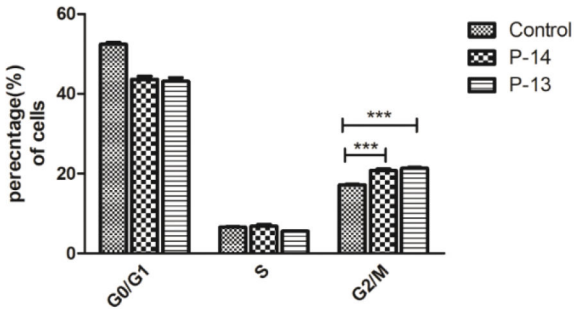

	Control	Treatment-P14	Treatment-P13
G0/G1	52.43±0.76	43.60±1.39	43.11±1.60
S	6.56 ±0.24	6.85±0.68	5.56±0.03
G2/M	17.14 ±0.28	20.77±0.65	21.35±0.34

Figure 4.

Effects of pyrazolones P14 and P13 on the cell cycle progression of NCI-H522 cells, *** represents p-value< 0.001.

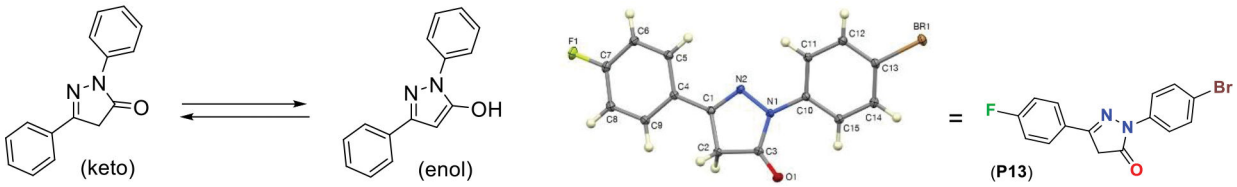

Figure 5.
Keto-enol forms of pyrazolones and keto-form preference in solid state.

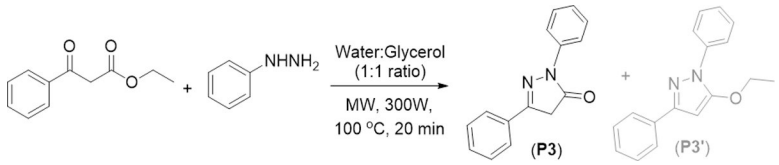

Scheme 1.

Microwave assisted synthesis of 1,3-diphenyl pyrazol-5-one **P3**

Table 1.

Microwave assisted synthesis of 1,3-disubstituted pyrazol-5-ones

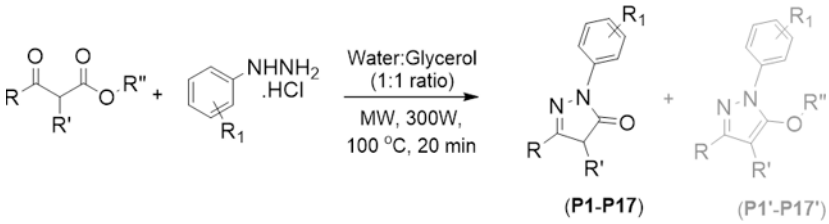

Code	structure	% Yield[a]
P1[b]	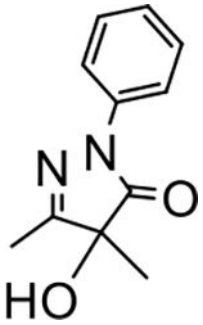	86
P2	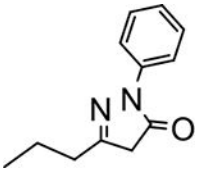	93
P3	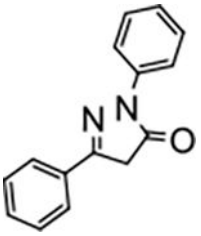	88
P4	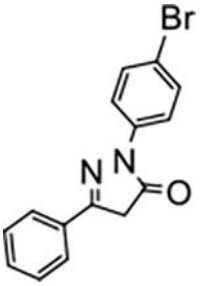	78 (91)[c]

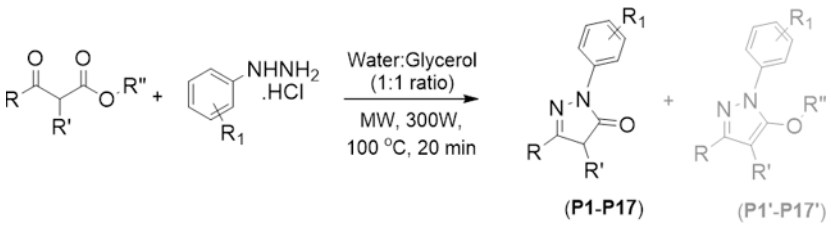

Code	structure	% Yield[a]
P5	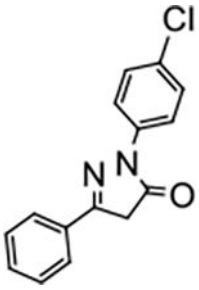	74 (88)[c]
P6	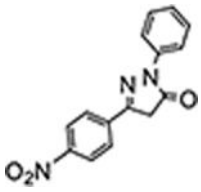	82
P7	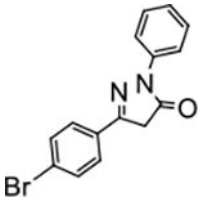	78
P8	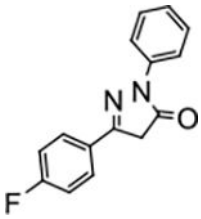	85
P9	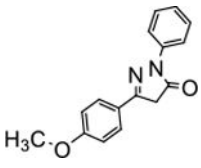	66

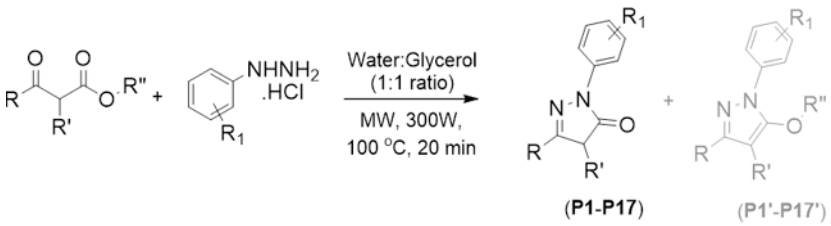

Code	structure	% Yield[a]
P10	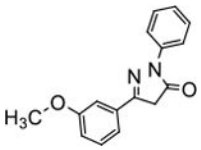	83
P11	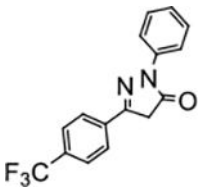	92
P12	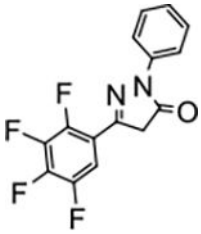	85
P13	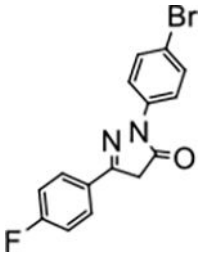	72 (86)[c]
P14	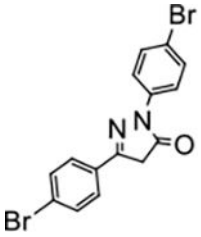	76 (89)[c]

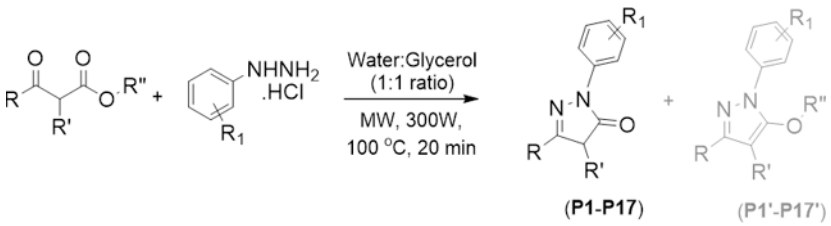

Code	structure	% Yield[a]
P15	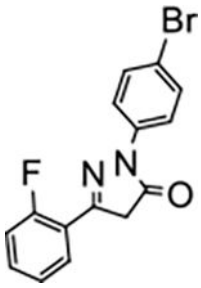	68 (82)[c]
P16	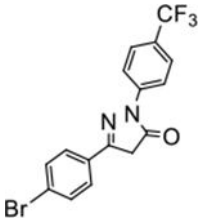	73
P17	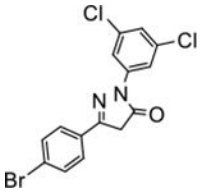	71

[a] isolated yields of pyrazolones

[b] areal C-H oxidation was observed

[c] isolated yields of pyrazolones after dealkylation

Table 2.

Antiproliferative activity of the synthesized pyrazolone compounds[a]

S. No.	IC_{50} μM		
	A549	**NCIH522**	**Non-cancerous HLF** [b]
PC-1[c]	8.46 ± 2.03	5.34 ± 0.94	12.15 ± 3.12
PC-2[c]	14.27 ± 4.20	13.86 ± 2.99	24.39 ± 2.16
P1	>100	>100	>100
P2	>100	>100	ND
P3	10.35 ± 1.55	17.01 ± 2.61	25.12 ± 1.39
P4	2.61± 1.12	4.93 ± 1.13	0.72± 1.07
P5	1.98± 1.10	4.50 ± 1.16	0.99± 1.25
P6	39.56± 1.05	40.5 ± 2.30	26.84± 1.40
P7	6.35 ± 0.85	4.70 ± 1.38	61.26 ± 1.08
P8	9.51±3.12	17.88 ±3.36	17.71 ± 1.10
P9	42.25 ± 2.76	51.25 ± 3.06	ND
P10	>100	>100	ND
P11	5.98±0.84	4.88±1.73	26.06 ± 1.12
P12	8.6 ± 0.59	9.9 ±2.44	8.52 ±1.09
P13	2.67± 0.51	3.70 ± 0.34	3.57 ±1.15
P14	2.73±0.28	2.41±0.57	2.55 ± 1.10
P15	3.58± 0.88	10.22 ± 1.30	1.07± 1.30
P15’	51.09 ± 1.14	61.70 ± 1.12	45.10 ± 1.15
P16	3.37 ± 0.10	2.95 ± 0.18	1.45 ±1.14
P17	5.56 ±0.07	5.07±1.18	6.94 ±1.12

[a]Each experiment was independently performed three times and values are represented ± SD

[b]non-cancerous human lung fibroblast cells

[c]PC = positive control (PC-1 = Afatinib, PC-2 = Gefitinib)